

ORIGINAL ARTICLE

Repeated mild traumatic brain injury results in long-term white-matter disruption

Virginia Donovan¹, Claudia Kim², Ariana K Anugerah², Jacqueline S Coats³, Udochuwku Oyoyo⁴, Andrea C Pardo³ and Andre Obenaus^{1,3}

Mild traumatic brain injury (mTBI) is an increasing public health concern as repetitive injuries can exacerbate existing neuropathology and result in increased neurologic deficits. In contrast to other models of repeated mTBI (rmTBI), our study focused on long-term white-matter abnormalities after bilateral mTBIs induced 7 days apart. A controlled cortical impact (CCI) was used to induce an initial mTBI to the right cortex of Single and rmTBI Sprague Dawley rats, followed by a second injury to the left cortex of rmTBI animals. Shams received only a craniectomy. *Ex vivo* diffusion tensor imaging (DTI), transmission electron microscopy (TEM), and histology were performed on the anterior corpus callosum at 60 days after injury. The rmTBI animals showed a significant bilateral increase in radial diffusivity (myelin), while only modest changes in axial diffusivity (axonal) were seen between the groups. Further, the rmTBI group showed an increased g-ratio and axon caliber in addition to myelin sheath abnormalities using TEM. Our DTI results indicate ongoing myelin changes, while the TEM data show continuing axonal changes at 60 days after rmTBI. These data suggest that bilateral rmTBI induced 7 days apart leads to progressive alterations in white matter that are not observed after a single mTBI.

Journal of Cerebral Blood Flow & Metabolism (2014) **34**, 715–723; doi:10.1038/jcbfm.2014.6; published online 29 January 2014

Keywords: axon caliber; bilateral injury; corpus callosum; diffusion tensor imaging; myelin

INTRODUCTION

Mild traumatic brain injury (mTBI) is a growing public health concern accounting for ~75% of all reported head injury cases.¹ After a concussive event a series of pathophysiologic processes ensue, including changes in metabolism, cerebral blood flow, and neurotransmission.² Despite these alterations most individuals appear to initially recover normally from mTBI, however several clinical studies have reported the presence of long-term emotional and cognitive sequelae after a single mild injury.^{3,4} In addition, several clinical and experimental studies provide evidence of increased brain vulnerability after a mild head injury in which a second mTBI may result in exacerbated tissue damage and neurologic deficits.^{5–8}

Little is understood about the underlying pathophysiology that leads to long-term deficits after repeated mTBI (rmTBI). Clinically, patients sustaining a second mild injury 10 to 13 days after an initial concussion showed prolonged alterations in brain metabolites (*N*-acetylaspartate-to-creatine ratio) compared with those individuals only experiencing a single injury.⁷ Experimentally, animal models in which injuries were induced to the same anatomic location revealed a time window of vulnerability, in which a second injury within 3 days of the first exacerbated ongoing metabolic, behavioral, and tissue changes.^{6,8–12} These outcomes were not observed if a second mTBI was induced 5 to 7 days after an initial insult, suggesting that no cumulative injury occurs when the temporal interval is sufficiently large.^{6,8,12} However, we have previously reported that rmTBI induced to

different anatomic locations did not result in exacerbated damage when injuries were spaced 3 days apart, but brain vulnerability such as increased bleeding was apparent when a second injury was induced 7 days after the initial insult.⁵ These data suggest that the susceptibility of the brain to subsequent injuries may be dependent on both the time interval between and the anatomic locations of mTBIs.

White matter is particularly vulnerable to mTBI and damage to fiber tracts is believed to have a role in the development of neurologic and cognitive deficits, which can develop slowly and persist for years after human concussion.¹³ Difficulties in clinical evaluation of white-matter integrity have led to the development of diffusion tensor imaging (DTI) to noninvasively detect myelin and axon pathology.^{14–17} Diffusion tensor imaging quantifies the directionality of water diffusion, which moves preferentially along white-matter fibers with reduced movement perpendicular to axonal orientation due to cellular barriers, such as the myelin sheath and cytoskeletal structures.¹⁸ A number of measures can be derived from DTI, including axial (AD) and radial (RD) diffusivities, which often correlate with axonal and myelin integrity, respectively. Clinically, white-matter DTI imaging of mild and moderate TBI has revealed that both injury types can result in altered water diffusion along fiber tracts.^{13,14,16} Further, DTI changes have also been reported in a study of athletes sustaining repeated subconcussive head injuries, indicating that even minimal trauma may result in long-term white-matter alterations.¹⁹ Animal models of mTBI have shown reduced RD at

¹Cell, Molecular and Developmental Biology Program, University of California, Riverside, California, USA; ²School of Medicine, Loma Linda University, Loma Linda, California, USA;

³Department of Pediatrics, Loma Linda University, Loma Linda, California, USA and ⁴Department of Radiology, Loma Linda University, Loma Linda, California, USA.

Correspondence: Dr A Obenaus, Department of Pediatrics, Loma Linda University, 11175 Campus Street, Room A1120, Loma Linda, CA 92354, USA.

E-mail: aobenaus@llu.edu

This study was supported by funding from the Department of Defense (DCMRP #DR080470 to AO) and in part by the National Science Foundation Integrative Graduate Education and Research Traineeship (IGERT) in Video Bioinformatics (DGE 0903667 to VD).

Received 17 July 2013; revised 18 December 2013; accepted 23 December 2013; published online 29 January 2014

7 and 30 days after experimental blast injury, suggesting that myelin disruption evolves after mild injuries.²⁰ Interestingly, in a closed head injury model of rmTBI, induced 1 day apart to the same anatomic location, no DTI changes were detected immediately after the second injury, while reduced AD was observed 7 days later illustrating the progressive nature of head injuries.²¹ Other experimental studies using moderate TBI models have reported acute decreases in AD followed by delayed increases in RD 1 to 4 weeks after injury, suggesting that the evolution of white-matter injury begins with axonal damage followed by later disruptions in myelin integrity.^{17,22–24} However, the development of white-matter damage after single and repeated mTBI is not well understood and further investigations are needed. It is also important to note that the evolution of white-matter pathology in these various models of TBI is likely different and is not well understood. Further investigations are required to better understand the development of white-matter damage after single and repeated mTBI.

An early histologic study of patients experiencing mTBI found axonal swelling within the corpus callosum (CC) and hippocampal white matter (fornices) up to 99 days after injury.²⁵ Surprisingly, there have been few long-term experimental mTBI studies that have evaluated both axonal and myelin damage after injury. Predominantly, animal studies have focused on axonal damage after mTBI, reporting early axonal transport abnormalities within 14 days of injury that appeared to pseudo-normalize by 4 weeks in the absence of myelin changes.^{26–28} Additionally, animal models of rmTBI have reported white-matter abnormalities at 7 days and up to 7 weeks after injury.^{10,11,21} These studies, however, focused primarily on white-matter changes at sites underneath the impact, despite the widespread damage that is often seen after human concussion.¹³ Other models of trauma investigating secondary degeneration using optic nerve transection have observed chronic axonal swelling and defects in myelin compaction within regions spatially distant from the injury site.²⁹ Due to the vulnerability of white matter to mTBI and the observed evolution of pathology after injury, analysis of regions distant from the impact site can be useful in assessing the spatial and temporal effects of single and repeated mTBIs.

Experimental studies of rmTBI, especially those in which injuries are induced to different anatomic locations, are critical to understand the clinical consequences of repeated injuries on white-matter integrity. Furthermore, due to the evolving nature of mTBI, long-term studies evaluating tissue distant from the injury site are warranted to better understand how the progression of white-matter disruption contributes to the long-term clinical observations of neurologic deficits. The purpose of our study was to evaluate long-term axonal and myelin damage within the anterior CC, a region which was not directly under the impact site, after rmTBI in which injuries were induced to contralateral locations 7 days apart. We tested the hypothesis that rmTBI results in long-term myelin disruption with little evidence of axonal changes at 60 days after injury.

MATERIALS AND METHODS

The manuscript was written in accordance with the ARRIVE guidelines. All experiments and care for animals were approved by the Loma Linda University Institutional Review Board and were conducted according to the principles and procedures of the Guidelines for Care and Use of Experimental Animals.

Controlled Cortical Impact

Male Sprague Dawley rats (Harlan Laboratories, Placentia, CA, USA; $n = 21$) ages 2 to 4 months (300 to 400 g) were housed on a 12-hour light/dark cycle in a temperature controlled animal facility. Animals were randomly assigned to three experimental groups: Sham controls, Single mTBI, and rmTBI induced 7 days apart (Figure 1A). The controlled cortical impact (CCI)

method was used to induce mild injuries as previously described.⁵ Briefly, a midline incision exposed the skull surface of anesthetized rats and a 5-mm craniectomy was performed over the right hemisphere 3 mm posterior and 3 mm lateral from Bregma (Figure 1B). A mild CCI (4 mm diameter tip, 0.5 mm depth, 6.0 m/s speed, 200 ms dwell) was then delivered to the cortical surface using an electromagnetically driven piston. The rmTBI group received a second craniectomy and mild CCI to the left cortical surface using identical parameters and coordinates as the first injury (Figures 1A and 1B). Sham controls underwent a single craniectomy and did not receive a CCI. Animals were then randomly assigned to either magnetic resonance imaging + histology ($n = 4$ /group) or transmission electron microscopy (TEM; $n = 3$ /group).

Ex Vivo Magnetic Resonance Imaging and Analysis

Animals were killed via transcardial perfusion using 4% paraformaldehyde 60 days (60 to 65 days) after the initial injury.³⁰ Extracted brains were then postfixed in 4% paraformaldehyde overnight and underwent two 30-minute washes in $1 \times$ phosphate-buffered saline after postfixation. The DTI and T2 weighted imaging (T2WI) data were collected at room temperature with a 256×256 matrix, 2 cm field of view and 1 mm slice thickness from *ex vivo* brains using an 11.7T Bruker Avance instrument (Bruker Biospin, Billerica, MA, USA). T2WIs were acquired with repetition time/echo time = 1,769.9/10.2 ms and DTI was acquired from a total of seven directions using a spin-echo diffusion sequence (repetition time/echo time = 552.5 ms/15.1 ms) with a single b_0 value ($b_0 = 43.3$ seconds/ mm^2) and six weighted DTI images ($b = 2,013.3$ seconds/ mm^2).

The anterior (bregma, -1.0 to $+0.5$ mm) CC was chosen for evaluation because it was not directly under the impact site (Figure 1C). The anterior CC was manually outlined on three consecutive T2WI slices using the Cheshire image processing software (Hayden Image/Processing Group, Waltham, MA, USA) by investigators blinded to group allocation. The midline and third ventricles were used to identify and facilitate segmentation of the right and left CC regions of interest (ROIs) (Figure 1C, left). To examine regionally distinct CC changes, the center slice was used to separate the CC into 12 ROIs (6 each bilaterally) along the medial-lateral axis. These regional ROIs were drawn on T2WIs using boundaries defined by the orientation of white-matter fibers observed within relative anisotropy (RA) color maps of Sham animals (Figure 1C, right). To account for size and shape differences after injury, the RA color maps of injured animals were also used to facilitate manual segmentation. Since all T2 and DTI images were acquired using the same geometry, ROIs drawn on T2WIs were copied directly to the exact DTIs and data means were extracted for AD and RD ($\mu\text{m}^2/\text{ms}$). The AD, RD, and RA were derived using the software written in Matlab (MathWorks, Natick, MA, USA) as previously described.³¹

Tissue Preparation for Histology

After magnetic resonance imaging, three of four brains from each group were randomly selected, as this was the minimum number of animals needed for statistical testing, and prepared for cryosectioning as previously described.³⁰ Briefly, brains were placed in 30% sucrose and embedded in optimal cutting temperature compound (OTC, Tissue Tek; Sakura Fine Tek, Torrance, CA, USA). Coronal sections ($30 \mu\text{m}$) were then either mounted directly on gelatin-chrome-alum-coated slides for Luxol fast blue (LFB) staining (stored at -20°C) or were free floating (stored in a cryoprotectant solution at 4°C) for immunohistochemistry.

Luxol Fast Blue Staining and Quantification

Luxol fast blue staining was performed on a minimum of three adjacent sections centered within the anterior CC to evaluate changes in structural integrity. Staining was performed as previously described with modifications.³² Briefly, mounted slices were thawed to room temperature for 30 minutes and placed into a 0.1% LFB staining solution (Solvent Blue 38 in 95% alcohol and 0.5% acetic acid) overnight at 56°C . Excess stain was removed by 95% alcohol and distilled water rinses for 1 minute each. Stained slices then underwent alternating 1 minute immersions in 0.05% lithium carbonate and 70% alcohol solutions for ~ 10 minutes. Subsequently, distilled water and 95% alcohol washes were performed for 1 minute each. Slices were then cleared using histoclear (National Diagnostics Inc., Charlotte, NC, USA) and coverslipped with permount mounting medium (Fisher Scientific, Fairlawn, NJ, USA).

Slices stained with LFB were imaged on an Olympus BX-51 microscope (Olympus, Center Valley, PA, USA) using the same imaging parameters ($\times 1.25$ objective, 1 second exposure) and illumination. Quantification of

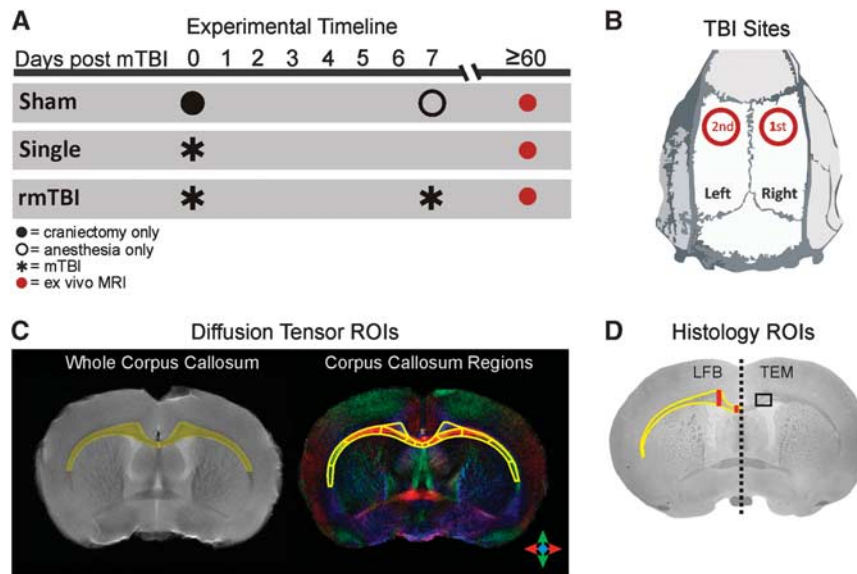


Figure 1. Experimental design and region of interest analysis. **(A)** A mild traumatic brain injury (mTBI) (denoted as *) was induced to the right cortex of all injured animals, while Sham controls only received a craniectomy ($n = 4$ per group). A second mTBI was then induced to the left cortex of rmTBI animals 7 days later (*). All animals were killed at 60 days after initial injury and *ex vivo* diffusion tensor imaging (DTI) was performed. **(B)** Schematic of the first (right) and second (left) mTBI locations. **(C)** DTI images were analyzed using the whole right and left corpus callosum (CC; left, yellow regions of interest (ROIs)). The CC was then examined using a total of 12 ROIs (6 each bilaterally) as shown on the relative anisotropy color maps, which depict the directionality of water diffusion along the CC (red: medial-lateral; green: dorsal-ventral; blue: anterior-posterior). **(D)** Changes in CC integrity were further examined using Luxol fast blue (LFB; $n = 3$ per group) staining and transmission electron microscopy (TEM; $n = 3$ per group). The area of the whole right and left CC (yellow ROI), cingulum (cingulum + CC) width, and midline CC width (red boxes) was measured in addition to LFB staining intensity. TEM analysis was performed on the right CC of Single and Sham animals and the left CC of rmTBI animals (black box denotes CC region). MRI, magnetic resonance imaging.

myelin integrity was performed by investigators blinded to group allocation using the Cheshire image processing software. Measures taken included the right and left staining intensity, area (mm^2), and width (mm) of the whole CC, cingulum (cingulum + CC), and CC adjacent to the midline (Figure 1D). The right and left area and width measurements were normalized to the respective right or left brain hemisphere area (mm^2), to account for any differences in hemispheric size between animals. All sections were stained simultaneously, but staining intensities for each right and left CC were normalized to that in the piriform cortex.

Immunohistochemistry and Analysis

Tissue sections centered in the anterior CC underwent immunohistochemistry as previously described.³⁰ Briefly, free floating sections were labeled with anti-rabbit NF200 (Sigma-Aldrich, St. Louis, MO, USA; 1:1,000) primary antibody at 4°C overnight to assess axonal integrity. Sections were then stained with goat anti-rabbit rhodamine (Millipore, Temecula, CA, USA; 1:1,000) secondary antibody for 1.5 hours at room temperature. After the staining procedure, slices were mounted onto gelatin-chrome-alum-coated slides using Vectashield hardset mounting medium (Vector Laboratories Inc., Burlingame, CA, USA). Negative controls omitted the primary antibody during the staining procedure.

Micrographs of NF200 immunolabeled tissue sections were taken with identical imaging parameters ($\times 20$, 1,000 ms exposure). ImageJ/Fiji³³ was used by investigators blinded to group allocation to detect the mean staining intensity of the right and left CC underneath the cingulum, CC adjacent to the midline, cingulum and cortex (above the cingulum).

Transmission Electron Microscopy and Quantification

Animals were perfused transcardially with $1 \times$ phosphate-buffered saline followed by a 2% glutaraldehyde (Electron Microscopy Sciences, Hatfield, PA, USA) and 2% paraformaldehyde in $1 \times$ phosphate-buffered saline fixative solution. Animals were decapitated and brains were initially postfixed *in situ* at 4°C overnight in the perfusion fixative, followed by further fixation of the extracted brains in 1% glutaraldehyde for ~3 days. The anterior brain region was cut coronally (~1 mm thick) allowing the CC (right CC of Single and Sham animals; left CC of rmTBI 7-day animals) to be identified under a dissecting scope. The CC was carefully dissected as a

$1 \times 2 \text{ mm}^2$ block 0.5 mm lateral from the midline to the end of the cingulum (Figure 1D). After extraction, the tissue blocks were then stored in $1 \times$ phosphate-buffered saline at 4°C for plastic embedding.

Tissue blocks were embedded in epon as previously described.³⁴ Briefly, blocks were fixed in 2% osmium tetroxide for 1 to 2 hours then rinsed in 0.1 mol/L cacodylate buffer followed by distilled water. After washing, blocks were stained overnight with 1% uranyl acetate at room temperature. Increasing concentrations of ethanol followed by propylene oxide were then used to dehydrate the tissue. Dehydrated tissue blocks were incubated in a 50/50 mixture of epon/propylene oxide for 3 to 4 hours, followed by an 80/20 epon/propylene mixture and then 100% epon overnight. After epon infiltration, the tissue blocks were placed in an embedding mold using 100% epon, which was polymerized through incubation at 60°C in an oven for 2 days.

Ultrathin sections were cut from the sample using a diamond knife on an ultramicrotome and mounted onto copper grids for TEM (JEOL, Peabody, MA, USA). Four random fields per grid from a total of two grids were analyzed per animal. Five random images within each field were collected at $\times 5,000$ and analyzed using ImagePro Plus (MediaCybernetics, Rockville, MD, USA) by an investigator blinded to group allocation. The axon and total fiber (axon + myelin) diameters were determined by taking the average of two separate measurements for every myelinated axon, from a minimum of 800 axons for each experimental group, where the entire axon had to be visible to be analyzed. The g-ratio was calculated for each myelinated axon by dividing the average axon diameter by the average total fiber diameter. The myelin thickness measurements were calculated by subtracting the total fiber and axon diameter measurements. Transmission electron microscopy analysis of the Single mTBI and rmTBI groups killed at 60 days after initial injury were compared with Sham controls 14 days after a craniectomy only.

Statistics

Statistical analysis was performed using SAS v9.1.3 (SAS, Cary, NC, USA) and Sigma Plot Software (Systat Software Inc., San Jose, CA, USA). Additionally, a power analysis was performed for each of the statistical tests and intraclass correlation coefficients were used to test for variability in ROI analysis using SAS v9.1.3 (Supplementary Tables 1 and 2). Results of the intraclass correlation testing revealed that AD (0.997), RD (0.891), and TEM

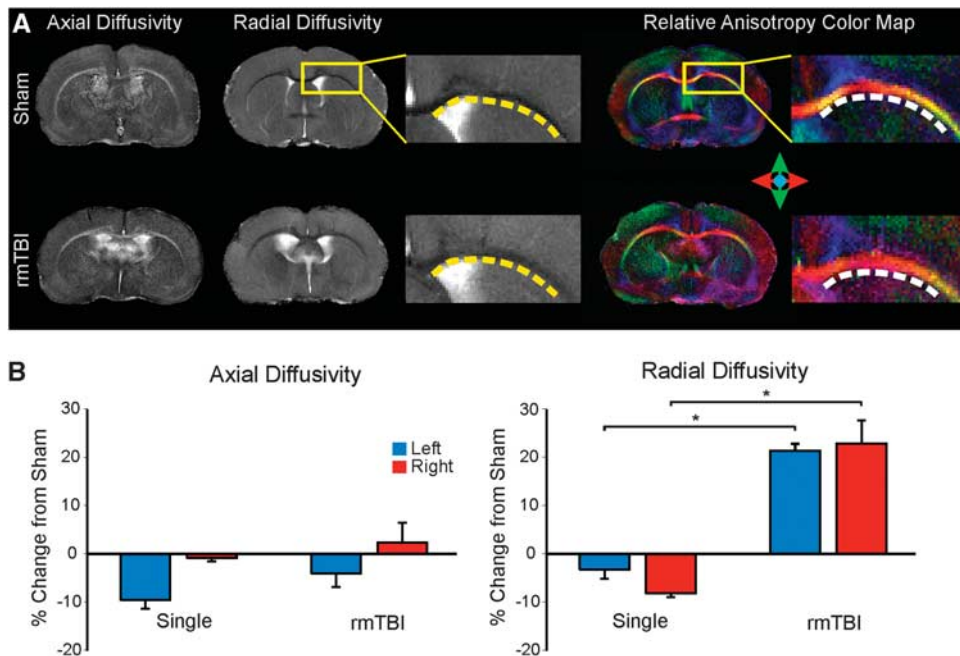


Figure 2. Radial diffusivity is increased in repeated mild traumatic brain injury (rmTBI) animals. (A) Representative diffusion tensor imaging (DTI) images illustrate changes in axial (AD) and radial (RD) diffusivities between Sham and rmTBI animals. The relative anisotropy (RA) color map reflects overall differences in water diffusion between the groups (red: medial-lateral; green: dorsal-ventral; blue: anterior-posterior). (B) Evaluation of AD revealed no significant differences between the injured groups within the right and left corpus callosum (CC). However, a significant increase ($*P < 0.001$) in RD was observed bilaterally within the rmTBI animals compared with the Single and Sham groups.

(0.981) ROIs were in agreement with each other (Supplementary Table 2). Data normality was assessed with the Kolmogorov–Smirnov or Shapiro–Wilk tests for each outcome variable and experimental group in each experiment. Whole CC DTI and histologic (LFB and NF200) data were compared among the control and experimental groups using the Generalized Linear Model procedure specifying an identity link function with a normal distribution. Using a one-way analysis of variance (ANOVA) with Bonferroni *post hoc* testing animal body weights were found to be significantly ($P < 0.001$) different between groups at the time of the initial injury; however, at the time of perfusion no differences ($P = 0.250$) in weights were found between groups. As a result, body weight at the time of the initial surgery in addition to the number of histologic sections (LFB 3 to 6 slices and NF200 1 to 2 slices) were included as covariates in statistical testing of the whole CC DTI and histologic data. Additionally, the DTI, LFB, and NF200 slices were treated independently as they spanned a large brain region. Analysis of the segmented CC DTI was performed using a two-way ANOVA with Bonferroni *post hoc* tests. Electron microscopy data (g-ratio, axon caliber, and myelin thickness) were tested using a Bonferroni repeated measures one-way ANOVA. Data are presented as the Mean \pm s.e.m. A $P < 0.05$ was considered as significant; P values were not adjusted for multiple tests.

RESULTS

Repeated Mild Traumatic Brain Injury Results in Chronic Myelin Disruption Within the Corpus Callosum

The right and left CC showed modest visible AD differences between groups, while dramatic changes were observed in the RD images of rmTBI animals compared with Shams (Figure 2A; left yellow box). Additionally, RA color maps from rmTBI animals confirmed disrupted water diffusion along the CC fibers compared with Shams, suggesting ongoing disruption within the CC (Figure 2A; right yellow box).

Quantification of AD revealed that Single and rmTBI groups did not exhibit a significant ($P > 0.50$) difference in AD within the whole right or left CC (Figure 2B; Supplementary Table 3); no significant differences were observed between the AD estimates of Sham controls and injured groups ($P > 0.13$) (Figure 2B;

Supplementary Table 3). Thus, axonal changes were not prominent at 60 days after injury on DTI. In contrast, a $> 16\%$ bilateral increase ($P < 0.001$) in RD was observed in the rmTBI group compared with Sham and Single animals, suggesting that a second mTBI 7 days later results in long-term and progressive myelin changes (Figure 2B; Supplementary Table 3). Importantly, at 60 days after injury these elevations in RD were found to be equally bilateral with no differences ($P > 0.50$) between the left and right CC of rmTBI animals. Further, no differences in RD were observed between the Sham and Single mTBI groups (Figure 2B; Supplementary Table 3).

Myelin Disruption Is Observed Globally Throughout the Corpus Callosum

To determine whether there was regional vulnerability within the CC, a segmented regional analysis of the right (first surgery site) and left (second surgery site) CC was undertaken (Figure 3A). Statistical analysis did not find any significant differences along the medial-lateral extent of the CC for AD or RD measurements (Figures 3B and 3C; Supplementary Tables 4 and 5). Additionally, quantification of NF200 staining intensity revealed no differences between groups, indicating that axonal neurofilaments did not appear to be affected long-term (data not shown). Interestingly, each of the rmTBI CC segmented regions, including the cingulum, showed an elevated RD compared with other groups suggesting that myelin disruption is widespread and that not any single region of the CC predominantly contributes to the overall increase in RD observed within the whole CC analysis (Figures 2B and 3C; Supplementary Table 5).

Corpus Callosum Area Is Increased after Repeated Mild Traumatic Brain Injury

Gross morphologic evaluations of the CC were performed to assess myelin loss using LFB staining (Table 1). Quantitative analysis revealed significant increases ($P < 0.018$ left and $P < 0.001$

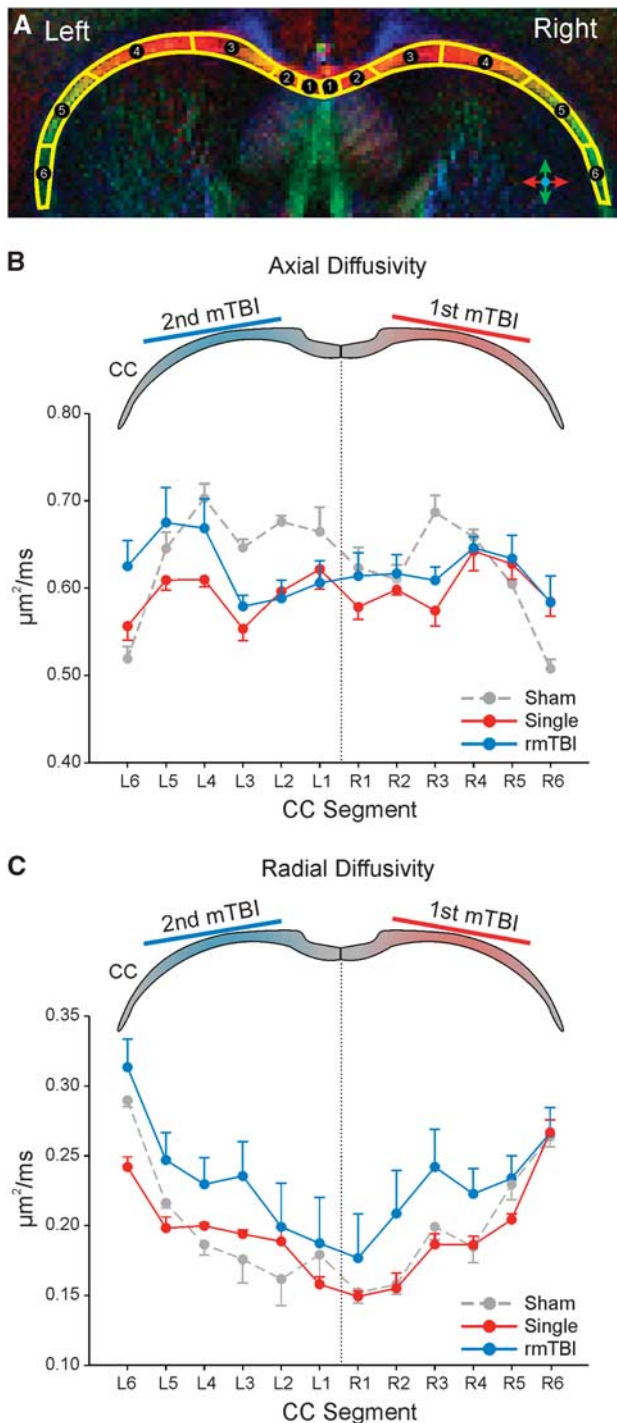


Figure 3. Radial diffusivity is elevated throughout the entire corpus callosum (CC) in repeated mild traumatic brain injury (rmTBI) animals. **(A)** Schematic depicting the right and left regions of interest (ROIs) used to further examine regional diffusion tensor imaging (DTI) changes within the CC (red: medial-lateral; green: dorsal-ventral; blue: anterior-posterior). **(B)** Axial diffusivity (AD) measurements revealed no significant changes between the groups within the right (first mTBI) or left (second mTBI) CC. **(C)** Radial diffusivity (RD) measurements taken from the segmented regions showed no significant differences between the experimental groups. However, the rmTBI animals showed elevated RD in every segment compared with the Sham and Single groups.

right) in the right and left CC area and midline CC width between the Single and rmTBI groups; however, no differences were found between injured animals and Sham controls (Table 1). Additionally, in the left cingulum (cingulum + CC) rmTBI animals showed increased ($P < 0.001$) widths compared with other groups, while in the right cingulum the rmTBI groups showed significant ($P = 0.009$) increases compared with Single animals only, suggesting that the CC size was enlarged at 60 days after injury (Table 1). Intensity of LFB staining was also significantly increased in the right CC, midline CC, and cingulum (cingulum + CC) in rmTBI animals compared with Shams (Table 1). However, the left CC and midline CC of rmTBI animals showed no differences from other groups, while the left cingulum (cingulum + CC) revealed a significant ($P = 0.032$) increase from Sham controls indicating that no myelin loss was detectable at this time point (Table 1).

White-Matter Ultrastructure Is Compromised after Repeated Mild Traumatic Brain Injury

Morphologic alterations were further explored through TEM analysis of CC ultrastructure at the site of the second injury in rmTBI animals and at the site of the first injury in the Single and Sham groups. Increased structural abnormalities were observed within myelinated axons of rmTBI animals compared with other groups (Figures 4A1–A3). While normal myelinated axons predominantly appeared within Shams as a compact sheath closely encompassing an axon (Figure 4B1), injured animals frequently showed various abnormalities including separation of myelin from the axon (Figure 4B2), decompaction of the myelin sheath (Figure 4B3), and fragmentation of the myelin sheath (Figures 4B4–B5).

G-ratio measurements were performed to quantify the observed abnormalities and revealed a significantly increased g-ratio in rmTBI animals compared with Sham ($P = 0.017$) and Single ($P = 0.007$) animals (Figure 4C). No g-ratio differences were observed between the Sham and Single groups (Figure 4C). We further assessed axonal caliber and myelin thickness separately to better identify their contributions to the g-ratio increases. Axonal caliber was significantly increased ($P < 0.001$) in rmTBI animals but significantly decreased ($P < 0.001$) in the Single group compared with Sham controls (Figure 4C). In contrast, myelin thickness (fiber diameter – axon diameter) revealed that both the Single and rmTBI groups were significantly ($P < 0.001$) decreased from Shams (Figure 4C). Thus, both increased axon caliber and decreased myelin thickness contributed to the observed increased g-ratio in rmTBI animals. Both measures were decreased in the Single mTBI group resulting in a similar g-ratio to those found in Shams.

DISCUSSION

Using macroscopic and ultrastructural approaches, we report long-term disruption in white matter distant from the injury site, providing new insights into the progression of white-matter alterations after rmTBI. Our novel findings include: (1) DTI evidence of ongoing widespread myelin disruption after rmTBI; (2) enlarged CC size in rmTBI animals, (3) increased myelin sheath decompaction, fragmentation, and separation from axons after repeated injuries, and (4) dramatic changes in rmTBI white-matter morphology, including increased axonal caliber and decreased myelin thickness at 60 days after rmTBI. Together, our findings show that rmTBI results in ongoing white-matter abnormalities at chronic time points in regions distant from the impact site.

Diffusion Tensor Imaging Identifies Long-Term Myelin Changes after Repeated Mild Traumatic Brain Injury

Previous studies using shiverer mice have shown that DTI measurements of AD and RD are good correlates of macroscopic axonal and myelin integrity, respectively.³⁵ *Ex vivo* studies have

Table 1. Luxol fast blue signal intensity and thickness measurements of corpus callosum regions

	Sham	Single	rmTBI	P value Sham vs. Single	P value Sham vs. rmTBI	P value Single vs. rmTBI
1a. Left corpus callosum						
<i>Whole CC</i>						
Area ^a (mm ²)	5.45 ± 3.6	5.22 ± 6.5	5.91 ± 11	P = 1.000	P = 0.532	P = 0.018
Signal intensity (AU)	0.91 ± 0.1	0.97 ± 0.1	0.98 ± 0.1	P = 0.558	P = 0.125	P = 1.000
<i>Midline CC</i>						
Width ^b (mm)	2.48 ± 2.1	2.34 ± 2.3	2.74 ± 4.3	P = 1.000	P = 0.208	P < 0.001
Signal intensity (AU)	1.02 ± 0.1	1.12 ± 0.1	1.10 ± 0.1	P = 0.011	P = 0.084	P = 1.000
<i>Cingulum</i>						
Width ^b (mm)	5.22 ± 4.8	4.69 ± 8.3	6.11 ± 5.4	P < 0.001	P < 0.001	P < 0.001
Signal intensity (AU)	0.93 ± 0.1	1.00 ± 0.1	1.01 ± 0.1	P = 0.186	P = 0.032	P = 1.000
1b. Right corpus callosum						
<i>Whole CC</i>						
Area ^a (mm ²)	5.53 ± 4.3	5.23 ± 5.5	6.08 ± 11	P = 1.000	P = 0.164	P = 0.001
Signal intensity (AU)	0.95 ± 0.1	1.01 ± 0.1	1.03 ± 0.1	P = 0.150	P = 0.005	P = 1.000
<i>Midline CC</i>						
Width ^b (mm)	2.58 ± 2.6	2.33 ± 1.4	2.71 ± 4.3	P = 0.069	P = 1.000	P < 0.001
Signal intensity (AU)	1.08 ± 0.1	1.16 ± 0.1	1.15 ± 0.1	P = 0.006	P = 0.032	P = 1.000
<i>Cingulum</i>						
Width ^b (mm)	5.33 ± 6.2	5.01 ± 12	6.19 ± 11	P = 1.000	P = 0.144	P = 0.009
Signal intensity (AU)	0.97 ± 0.1	1.03 ± 0.1	1.05 ± 0.1	P = 0.212	P = 0.005	P = 1.000

CC, corpus callosum; rmTBI, repeated mild traumatic brain injury. ^aArea = 10⁻² ± 10⁻³. ^bWidth = 10⁻⁴ ± 10⁻⁵.

shown that DTI measures extracted from white matter in perfusion fixed brains correlate with TEM and histologic measures.³⁶⁻³⁹

A number of studies comparing *in vivo* and *ex vivo* DTI measures (i.e., AD and RD) have revealed that *ex vivo* diffusivity measures are reduced compared with *in vivo* measures.³⁶⁻³⁸ However when compared with sham values, *ex vivo* RD measures provide reliable diffusivity changes reflecting ongoing pathology.³⁷ Additionally, several studies also note that AD measures were potentially not as reliable as those collected *in vivo*, possibly due to the type of ongoing axonal pathology.^{36,38} It is important to note that many of these DTI studies were performed in cuprizone and ischemia models, which result in white-matter pathology that is considerably different from that observed after mTBI.

Surprisingly, very few DTI studies have been performed in animal models of mTBI. In the anterior CC, 1 to 2 mm distant from the injury site, we observed a widespread bilateral increase in RD within rmTBI animals that was not seen after a single mTBI at 60 days after injury. Additionally, only modest AD changes were observed in rmTBI animals at this chronic time point. Similarly, a model of mild blast TBI also observed no changes in AD; however, this study also reported a decrease in RD within the hypothalamus and the thalamus at 7 and 30 days after injury.²⁰ While the axonal changes are consistent with our findings, the decreased myelin diffusivity at 7 and 30 days may reflect continued tissue swelling not observed at our late 60-day time point. Alternatively, the pathology that ensues after a diffuse blast injury is likely to be different from that after a focal TBI, thus resulting in different DTI outcomes. Interestingly, a model of rmTBI that induced two closed head injuries 1 day apart to the same anatomic location showed no AD or RD changes in the CC immediately after the second mTBI.²¹ However, 7 days after the initial injury decreases in AD were found within the CC, while no changes in RD were detected.²¹ Experimental differences, including location of injury, time interval between mTBI events and *ex vivo* as opposed to *in vivo* DTI measures, make it difficult to compare the study performed by Bennett *et al*²¹ and our own. However, their DTI data suggest that axonal damage occurs early in the absence of myelin changes, while our data indicate that myelin disruption is

more prominent at late times with little change in axonal integrity after rmTBI.

In contrast to experimental studies, DTI is increasingly being used in human research studies to detect and monitor the progression of white-matter damage after mild injuries. Several clinical studies have reported increased AD, often involving several white-matter structures throughout the brain of patients evaluated ~2 to 7 years after concussion.^{13,15} Though our injury model shows little axonal change at 60 days after rmTBI, this may be due to the focal nature of our TBI model, whereas human mTBI is typically more diffuse. Our AD assessment may be early compared with clinical studies, as our ultrastructural (TEM) findings suggest ongoing axonal pathology that could not be detected by DTI. Additionally, perfusion fixation could increase membrane permeability and increase protein crosslinking within axons that could potentially mask changes in AD typically seen within human subjects.^{36,38} Further, caution should be exercised, as a recent human study of multiple sclerosis in the spinal cord found that RD increased not only as a result of demyelination, but also as a result of axonal damage.⁴⁰ Nevertheless, our study provides insight into the ongoing white-matter damage that occurs after rmTBI, which potentially contributes to the delayed onset of neurologic deficits often seen after human concussion.

White-Matter Structure Is Damaged after Repeated Injuries

Healthy white matter has a g-ratio of 0.7 to 0.8, where a value of 1.0 may suggest overt demyelination or increased axonal caliber. Quantification of myelinated axon integrity revealed an increased g-ratio within rmTBI animals compared with other groups. To discriminate whether axon caliber or myelin thickness contributed to our increased g-ratio, we compared axon diameter and myelin (fiber-axon) thickness between our experimental groups. Within rmTBI animals, we observed a significant increase in axon caliber and a significant decrease in myelin thickness compared with Shams, suggesting that both enlarged axons and thinner myelin contribute to the increased g-ratio. Similar increases in axonal caliber have also been reported in TBI and optic nerve transection

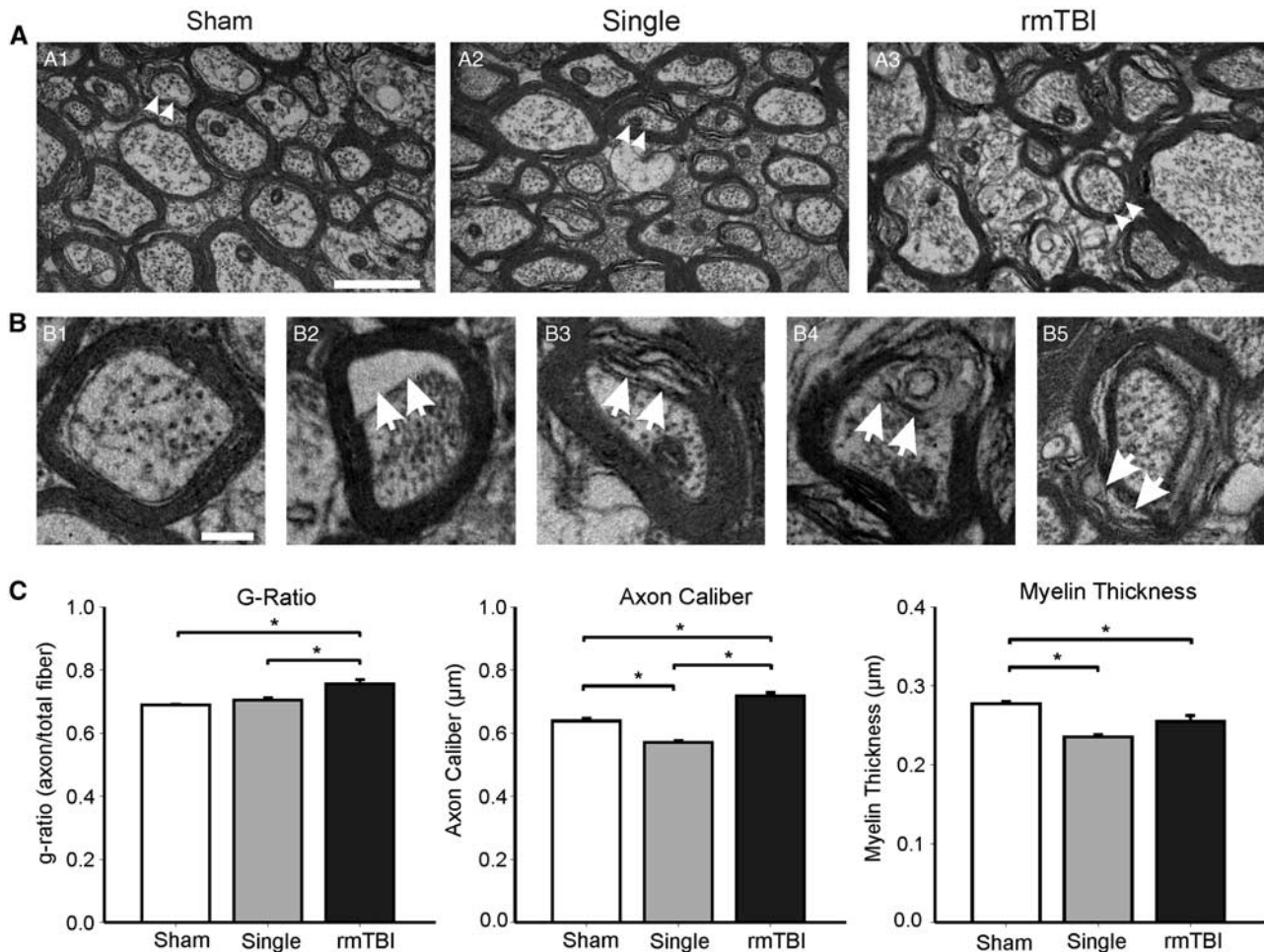


Figure 4. Ongoing white-matter damage is evident in the corpus callosum (CC). **(A)** Representative transmission electron microscopy (TEM) images illustrate increased white-matter abnormalities (arrows) within repeated mild traumatic brain injury (rmTBI) animals (A3) at the site of the second injury (left) compared with the site of first injury (right) within the Sham (A1) and Single (A2) groups; cal bar = 1 μm . **(B)** Normal myelinated axons appear with a tightly wrapped sheath located near the axon (B1). Typical abnormalities (arrows) within the CC included large separations of the myelin sheath from the axon (B2), breaking of the sheath layers (B3), and deterioration of the myelin (B4 and B5); cal bar = 0.2 μm . **(C)** The rmTBI group revealed a significant increase ($*P < 0.001$) in g-ratio (axon/fiber diameter) compared with other groups. Similarly, the axon caliber of rmTBI animals was also increased ($*P < 0.001$) compared with Sham and Single groups. The Single group also exhibited a significant decrease ($*P < 0.001$) in axon caliber compared with Shams. Both the Single and rmTBI groups showed a significant ($*P < 0.001$) decrease in myelin thickness compared with Sham animals.

studies, in regions both distant and adjacent to the injury site.^{29,41} Interestingly, both axon caliber and myelin thickness were significantly decreased in Single mTBI animals compared with Shams, indicating that after a mTBI surviving axons are smaller. Studies using spinal cord injury have observed axons with both increased and decreased axonal caliber within distinct anatomic locations surrounding the injured site.⁴² Our observed decrease in fiber size after a single mTBI may represent an alternate pathologic process from that seen after rmTBI.

Interestingly, our changes in axonal caliber were seen in the absence of neurofilament changes (NF200 staining). Microtubule disruption, in addition to neurofilament changes, has been previously shown to result in acute axonal swelling.⁴³ In our study, axonal neurofilaments may have recovered and thus appear to be stable at our late 60-day time point. Alternatively, the disruption in myelin structure and thus the disturbance to the axon–myelin relationship may result in morphologic changes as previous studies have shown that myelin has a role in regulating axonal cytoskeleton and overall caliber.⁴⁴ Irrespective of the putative evolution of white-matter pathology, at 60 days after

rmTBI there clearly is increased axonal size independent of neurofilament alterations.

To assess the contribution of myelin loss to our observed increase in RD, we stained tissue using LFB. We observed increases in LFB staining intensity and CC width within rmTBI animals compared with Shams. Similarly, a previous study using a model of juvenile TBI reported increased myelin basic protein staining at 60 days after a moderate TBI potentially as a result of myelin fragmentation.⁴⁵ Taken together with our TEM results, which show myelin thinning, increases in LFB staining may indicate increased myelin fragmentation within the CC that results in thinner myelin sheaths surrounding the axons. Observed increases in CC width however may reflect the increased axonal caliber seen in our ultrastructural TEM analysis. To date the majority of mTBI studies have focused on acute ultrastructural changes after injury. One long-term study after a single moderate TBI reported abnormalities in myelinated axon morphology at 3 months after injury with increased myelin debris and white-matter thinning in the external capsule at 6 to 9 months after injury.⁴¹ Though our LFB data are consistent with increased myelin debris seen in this study, we did

not observe white-matter thinning. However, several reasons exist for the discrepancies between this study and our own: (1) our study was only performed at 60 days after injury, (2) we utilized a mild injury, and (3) rmTBI could influence the temporal evolution of axonal and myelin damage. Other models of injury, such as partial optic nerve transection, have also reported abnormal myelin sheath compaction and axonal swelling in brain regions distant from the injury site 3 months later.²⁹ Our results reflect similar observations of structural abnormalities within the anterior CC, which was not underneath the impact site, suggesting that white-matter degeneration is ongoing in this model of rmTBI.

Potential Limitations and Caveats

One potential limitation of our study is the low animal numbers, which may potentially increase β -errors and render some tests statistically underpowered. However, we were able to reject the overall hypothesis of this study and we believe that through testing our hypothesis using several different complementary techniques that our results accurately reflect the ongoing pathology. It is also important to note experimental differences within our study, specifically that Single mTBI animals received only a single exposure of anesthesia, while the Sham and rmTBI groups underwent two anesthesia exposures. We chose not to perform a second craniectomy or bout of anesthesia on the Single group, as we wanted to compare the effects of single and repeated injuries. Further, though the Shams did receive two anesthesia exposures, an alternate cohort of Sham animals could have been subjected to a second craniectomy. This could potentially strengthen our findings associated with effects of rmTBI and future studies should include such a Sham group for comparison with experimental cohorts. Additionally in our TEM experiments, Shams were killed at 14 days rather than at the 60-day time point, as we believe that a single or double craniectomy alone would not have resulted in observable pathology at 60 days compared with that at 14 days. Analysis of CC area and signal intensity measured from LFB staining revealed no significant ($P \geq 0.258$) differences between Shams at 14 and 60 days after injury, indicating that no detectable structural or myelin changes were occurring temporally as a result of the craniectomy (data not shown). Nevertheless, it is important to realize that this could potentially influence our results as the craniectomy may result in acute transient ultrastructural changes in white-matter integrity at 14 days after injury that may mask the extent of damage occurring in mTBI 60-day animals.

CONCLUSION

Repeated mTBI compared with a single mTBI results in widespread alteration in CC integrity. We hypothesized that rmTBI would result in little axonal disruption, while myelin damage would be ongoing. While both our macroscopic (DTI) and ultrastructural (TEM) results support our hypothesis of ongoing myelin damage, unexpectedly the TEM data also showed that subtle axonal changes are still present at this late time point after rmTBI. These findings clearly show that rmTBI results in significantly increased long-term differences compared with a single mTBI. This raises significant clinical questions as to the long-term effects on white matter in individuals with rmTBI. Our experimental results provide a potential morphologic basis for many of the evolving abnormalities reported in clinical studies of mTBI. Further investigation of the relationship between myelin and axonal integrity after rmTBI is warranted to delineate the evolution of white-matter damage and to develop future therapeutics.

DISCLOSURE/CONFLICT OF INTEREST

The authors declare no conflict of interest.

ACKNOWLEDGMENTS

The authors wish to acknowledge Douglas Hauser, Ernesto Barron, and the USC/Norris Cancer Center's Cell and Tissue Imaging Core facility (supported by NCI grant P30CA014089) for assistance with TEM tissue preparation and imaging. Additionally, the authors would like to thank Dr Monica J Carson and Bethann Martinez for helpful suggestions and Faisal Rashid for assistance with manual segmentation of regional DTI ROIs. We also thank Dr Richard Sun for use of the DTI software and helpful discussions.

REFERENCES

- Faul M, Xu L, Wald MM, Coronado VG. *Traumatic Brain Injury in the United States: Emergency Department Visits, Hospitalizations and Deaths*. Centers for Disease Control and Prevention, National Center for Injury Prevention and Control: Atlanta, GA, 2010.
- Barkhoudarian G, Hovda DA, Giza CC. The molecular pathophysiology of concussive brain injury. *Clin Sports Med* 2011; **30**: 33–48vii–iii.
- Malojic B, Mubrin Z, Coric B, Susnic M, Spilich GJ. Consequences of mild traumatic brain injury on information processing assessed with attention and short-term memory tasks. *J Neurotrauma* 2008; **25**: 30–37.
- Konrad C, Geburek AJ, Rist F, Blumenroth H, Fischer B, Husstedt I *et al*. Long-term cognitive and emotional consequences of mild traumatic brain injury. *Psychol Med* 2010; **41**: 1–15.
- Donovan V, Bianchi A, Hartman R, Bhanu B, Carson MJ, Obenaus A. Computational analysis reveals increased blood deposition following repeated mild traumatic brain injury. *Neuroimage Clin* 2012; **1**: 18–28.
- Longhi L, Saatman KE, Fujimoto S, Raghupathi R, Meaney DF, Davis J *et al*. Temporal window of vulnerability to repetitive experimental concussive brain injury. *Neurosurgery* 2005; **56**: 364–374.
- Vagnozzi R, Signoretti S, Tavazzi B, Floris R, Ludovici A, Marziali S *et al*. Temporal window of metabolic brain vulnerability to concussion: a pilot 1H-magnetic resonance spectroscopic study in concussed athletes—part III. *Neurosurgery* 2008; **62**: 1286–1295.
- Vagnozzi R, Tavazzi B, Signoretti S, Amorini AM, Belli A, Cimatti M *et al*. Temporal window of metabolic brain vulnerability to concussions: mitochondrial-related impairment—part I. *Neurosurgery* 2007; **61**: 379–388.
- Tavazzi B, Vagnozzi R, Signoretti S, Amorini AM, Belli A, Cimatti M *et al*. Temporal window of metabolic brain vulnerability to concussions: oxidative and nitrosative stresses—part II. *Neurosurgery* 2007; **61**: 390–395.
- Laurer HL, Bareyre FM, Lee VM, Trojanowski JQ, Longhi L, Hoover R *et al*. Mild head injury increasing the brain's vulnerability to a second concussive impact. *J Neurosurg* 2001; **95**: 859–870.
- Shitaka Y, Tran HT, Bennett RE, Sanchez L, Levy MA, Dikranian K *et al*. Repetitive closed-skull traumatic brain injury in mice causes persistent multifocal axonal injury and microglial reactivity. *J Neuropathol Exp Neurol* 2011; **70**: 551–567.
- Huang L, Coats JS, Mohd-Yusof A, Yin Y, Assaad S, Muellner MJ *et al*. Tissue vulnerability is increased following repetitive mild traumatic brain injury in the rat. *Brain Res* 2013; **1499**: 109–120.
- Kinnunen KM, Greenwood R, Powell JH, Leech R, Hawkins PC, Bonnelle V *et al*. White matter damage and cognitive impairment after traumatic brain injury. *Brain* 2011; **134**: 449–463.
- Inglese M, Makani S, Johnson G, Cohen BA, Silver JA, Gonen O *et al*. Diffuse axonal injury in mild traumatic brain injury: a diffusion tensor imaging study. *J Neurosurg* 2005; **103**: 298–303.
- Kraus MF, Susmaras T, Caughlin BP, Walker CJ, Sweeney JA, Little DM. White matter integrity and cognition in chronic traumatic brain injury: a diffusion tensor imaging study. *Brain* 2007; **130**: 2508–2519.
- Kumar R, Husain M, Gupta RK, Hasan KM, Haris M, Agarwal AK *et al*. Serial changes in the white matter diffusion tensor imaging metrics in moderate traumatic brain injury and correlation with neuro-cognitive function. *J Neurotrauma* 2009; **26**: 481–495.
- Mac Donald CL, Dikranian K, Bayly P, Holtzman D, Brody D. Diffusion tensor imaging reliably detects experimental traumatic axonal injury and indicates approximate time of injury. *J Neurosci* 2007; **27**: 11869–11876.
- Niogi SN, Mukherjee P. Diffusion tensor imaging of mild traumatic brain injury. *J Head Trauma Rehabil* 2010; **25**: 241–255.
- Bazarian JJ, Zhu T, Blyth B, Borrino A, Zhong J. Subject-specific changes in brain white matter on diffusion tensor imaging after sports-related concussion. *Magn Reson Imaging* 2012; **30**: 171–180.
- Rubovitch V, Ten-Bosch M, Zohar O, Harrison CR, Tempel-Brami C, Stein E *et al*. A mouse model of blast-induced mild traumatic brain injury. *Exp Neurol* 2011; **232**: 280–289.
- Bennett RE, Mac Donald CL, Brody DL. Diffusion tensor imaging detects axonal injury in a mouse model of repetitive closed-skull traumatic brain injury. *Neurosci Lett* 2012; **513**: 160–165.

- 22 Li J, Li XY, Feng DF, Gu L. Quantitative evaluation of microscopic injury with diffusion tensor imaging in a rat model of diffuse axonal injury. *Eur J Neurosci* 2011; **33**: 933–945.
- 23 Li S, Sun Y, Shan D, Feng B, Xing J, Duan Y *et al*. Temporal profiles of axonal injury following impact acceleration traumatic brain injury in rats—a comparative study with diffusion tensor imaging and morphological analysis. *Int J Legal Med* 2013; **127**: 159–167.
- 24 Mac Donald CL, Dikranian K, Song SK, Bayly PV, Holtzman DM, Brody DL. Detection of traumatic axonal injury with diffusion tensor imaging in a mouse model of traumatic brain injury. *Exp Neurol* 2007; **205**: 116–131.
- 25 Blumbergs PC, Scott G, Manavis J, Wainwright H, Simpson DA, McLean AJ. Staining of amyloid precursor protein to study axonal damage in mild head injury. *Lancet* 1994; **344**: 1055–1056.
- 26 Creed JA, DiLeonardi AM, Fox DP, Tessler AR, Raghupathi R. Concussive brain trauma in the mouse results in acute cognitive deficits and sustained impairment of axonal function. *J Neurotrauma* 2011; **28**: 547–563.
- 27 Spain A, Dumas S, Lifshitz J, Rhodes J, Andrews PJ, Horsburgh K *et al*. Mild fluid percussion injury in mice produces evolving selective axonal pathology and cognitive deficits relevant to human brain injury. *J Neurotrauma* 2010; **27**: 1429–1438.
- 28 Shultz SR, MacFabe DF, Foley KA, Taylor R, Cain DP. A single mild fluid percussion injury induces short-term behavioral and neuropathological changes in the Long-Evans rat: support for an animal model of concussion. *Behav Brain Res* 2011; **224**: 326–335.
- 29 Payne SC, Bartlett CA, Harvey AR, Dunlop SA, Fitzgerald M. Chronic swelling and abnormal myelination during secondary degeneration after partial injury to a central nervous system tract. *J Neurotrauma* 2011; **28**: 1077–1088.
- 30 Obenaus A, Robbins M, Blanco G, Galloway NR, Snissarenko E, Gillard E *et al*. Multi-modal magnetic resonance imaging alterations in two rat models of mild neurotrauma. *J Neurotrauma* 2007; **24**: 1147–1160.
- 31 Sun SW, Liang HF, Le TQ, Armstrong RC, Cross AH, Song SK. Differential sensitivity of in vivo and ex vivo diffusion tensor imaging to evolving optic nerve injury in mice with retinal ischemia. *Neuroimage* 2006; **32**: 1195–1204.
- 32 Kluver H, Barrera E. A method for the combined staining of cells and fibers in the nervous system. *J Neuropathol Exp Neurol* 1953; **12**: 400–403.
- 33 Schindelin J, Arganda-Carreras I, Frise E, Kaynig V, Longair M, Pietzsch T *et al*. Fiji: an open-source platform for biological-image analysis. *Nat Methods* 2012; **9**: 676–682.
- 34 Mnatsakanyan L, Ross-Cisneros FN, Carelli V, Wang MY, Sadun AA. Axonal degeneration in peripheral nerves in a case of Leber hereditary optic neuropathy. *J Neuroophthalmol* 2011; **31**: 6–11.
- 35 Song SK, Sun SW, Ramsbottom MJ, Chang C, Russell J, Cross AH. Demyelination revealed through MRI as increased radial (but unchanged axial) diffusion of water. *Neuroimage* 2002; **17**: 1429–1436.
- 36 Sun SW, Liang HF, Xie M, Oyoyo U, Lee A. Fixation, not death, reduces sensitivity of DTI in detecting optic nerve damage. *Neuroimage* 2009; **44**: 611–619.
- 37 Sun SW, Neil JJ, Song SK. Relative indices of water diffusion anisotropy are equivalent in live and formalin-fixed mouse brains. *Magn Reson Med* 2003; **50**: 743–748.
- 38 Zhang J, Jones MV, McMahon MT, Mori S, Calabresi PA. In vivo and ex vivo diffusion tensor imaging of cuprizone-induced demyelination in the mouse corpus callosum. *Magn Reson Med* 2012; **67**: 750–759.
- 39 Leigland LA, Budde MD, Cornea A, Kroenke CD. Diffusion MRI of the developing cerebral cortical gray matter can be used to detect abnormalities in tissue microstructure associated with fetal ethanol exposure. *Neuroimage* 2013; **83**: 1081–1087.
- 40 Klawiter EC, Schmidt RE, Trinkaus K, Liang HF, Budde MD, Naismith RT *et al*. Radial diffusivity predicts demyelination in ex vivo multiple sclerosis spinal cords. *Neuroimage* 2011; **55**: 1454–1460.
- 41 Rodriguez-Paez AC, Brunschwig JP, Bramlett HM. Light and electron microscopic assessment of progressive atrophy following moderate traumatic brain injury in the rat. *Acta Neuropathol* 2005; **109**: 603–616.
- 42 Nashmi R, Fehlings MG. Changes in axonal physiology and morphology after chronic compressive injury of the rat thoracic spinal cord. *Neuroscience* 2001; **104**: 235–251.
- 43 Tang-Schomer MD, Johnson VE, Baas PW, Stewart W, Smith DH. Partial interruption of axonal transport due to microtubule breakage accounts for the formation of periodic varicosities after traumatic axonal injury. *Exp Neurol* 2012; **233**: 364–372.
- 44 Schnaar RL, Lopez PH. Myelin-associated glycoprotein and its axonal receptors. *J Neurosci Res* 2009; **87**: 3267–3276.
- 45 Ajao DO, Pop V, Kamper JE, Adami A, Rudbeck E, Huang L *et al*. Traumatic brain injury in young rats leads to progressive behavioral deficits coincident with altered tissue properties in adulthood. *J Neurotrauma* 2012; **29**: 2060–2074.

Supplementary Information accompanies the paper on the Journal of Cerebral Blood Flow & Metabolism website (<http://www.nature.com/jcbfm>)